1994-04

The Role of Edges and Line-Ends in Illusory Contour Formation

THE ROLE OF EDGES AND LINE-ENDS IN ILLUSORY CONTOUR FORMATION

Gregory W. Lesher and Ennio Mingolla

April 1994

Technical Report CAS/CNS–93–061

Boston University Center for Adaptive Systems and
Department of Cognitive and Neural Systems
111 Cummington Street
Boston, MA 02215

The Role of Edges and Line-Ends in Illusory Contour Formation

Gregory W. Lesher*

Ennio Mingolla†

Center for Adaptive Systems and
Department of Cognitive and Neural Systems
Boston University
111 Cummington Street
Boston, Massachusetts 02215 USA

* Supported in part by the Air Force Department of Scientific Research (AFOSR F49620-92-J-0334) and a National Science Foundation Graduate Fellowship.

† Supported in part by the Air Force Department of Scientific Research (AFOSR URI 90-0175 and AFOSR F49620-92-J-0334) and the Office of Naval Research (N00014-91-J-4100).

Abstract

Illusory contours can be induced along directions approximately collinear to edges or approximately perpendicular to the ends of lines. Using a rating scale procedure we explored the relation between the two types of inducers by systematically varying the thickness of inducing elements to result in varying amounts of "edge-like" or "line-like" induction. Inducers for our illusory figures consisted of concentric rings with arcs missing. Observers judged the clarity and brightness of illusory figures as the number of arcs, their thicknesses, and spacings were parametrically varied. Degree of clarity and amount of induced brightness were both found to be inverted-U functions of the number of arcs. These results mandate that any valid model of illusory contour formation must account for interference effects between parallel lines or between those neural units responsible for completion of boundary signals in directions perpendicular to the ends of thin lines. Line width was found to have an effect on both clarity and brightness, a finding inconsistent with those models which employ *only* completion perpendicular to inducer orientation.

Introduction

In two recent parametric studies of factors supporting illusory contour formation, Shipley and Kellman (1992a) and Banton and Levi (1992) reported that the ratio of the length of an illusory contour to the entire length of a contour composed of inducer segments and illusory segments was a prime factor in determining the perceived salience of the illusory contour. We say an illusory contour is *supported* where real luminance gradients specify its location. Thus we refer to the ratio of "real to illusory-plus-real length" as the *support ratio* of an illusory figure. Shipley and Kellman's and Banton and Levi's experiments employed solid "pacman" inducers, consisting of dark discs with a quarter missing (Kanizsa, 1955). Contour salience was found to be a monotonically increasing function of the support ratio for stimuli across a range of retinal size and inducer spacing. Our experiment employed similar illusory squares, but each inducer was composed of a number of concentric circles (with missing arcs), where both the width and number of lines (arcs) were varied.

In our study stimuli equivalent to those of Shipley and Kellman (1992a) and Banton and Levi (1992) represented a limiting case on the related dimensions of number of lines and line spacing. While our findings confirm the importance of the variable (support ratio) that these researchers investigated for illusory contour salience, we found clarity of the illusory contour, as well as brightness of the induced square, to be an *inverted-U function* of the support ratio rather than a monotonically increasing function. Further, a similar curve was generated as a function of the number of lines. That is, unlike the findings of Petry, Harbeck, Conway, and Levey (1983), who performed similar experiments with Ehrenstein type stimuli, more lines are not always better. The type of parametric data generated by these experiments are important in that they help to reveal the structure of the underlying mechanisms for illusory contour formation. The implications of our findings for the models of Finkel and Edelman (1989), Grossberg and Mingolla (1985a,b, 1987a,b), Kellman and Shipley (1991; Shipley & Kellman, 1990, 1992a,b), and Peterhans, von der Heydt, and Baumgartner (1986) are discussed.

Background

In a series of important neurophysiological experiments probing the early stages of illusory contour formation, von der Heydt, Peterhans, and Baumgartner (1984; Peterhans, von der Heydt, & Baumgartner, 1986; Peterhans & von der Heydt, 1989; von der Heydt & Peterhans, 1989) found neural responses to stimuli that yield illusory contours in humans in some V2 (but not V1) cells of alert rhesus monkeys. On the other hand, cognitive factors are undeniably important in modulating the strength of illusory contours, as demonstrated by the effect of perceptual set and memory on contour perception (Bradley & Petry, 1977; Rock & Anson, 1979; Wallach & Slaughter, 1988). That single-cell responses to illusory contours are present as early as V2, however, casts doubt on the necessity of postulating a central role for cognitive factors in illusory contour *formation* (Coren, 1972; Gregory, 1972; Kanizsa, 1979; Rock & Anson, 1979). On the psychophysical side, illusory and real contours have been shown to play similar functional roles in several phenomena of early vision, including tilt aftereffect (Smith & Over, 1975, 1976, 1977), apparent motion (von Grunau, 1979; Ramachandran, 1986), orientation discrimination (Vogels and Orban,

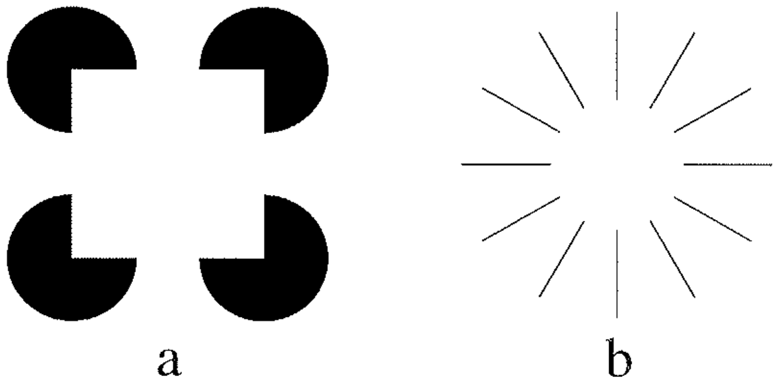

Figure 1: **(a)** Contour induction parallel to edges **(b)** Contour induction perpendicular to line-ends

1987), and motion aftereffect (Smith and Over, 1979; Weisstein, Maguire, & Berbaum, 1977), further supporting the hypothesis of a relatively early physiological instantiation of illusory contour formation. Our experiment was designed to parametrically characterize stimulus relations conducive to stronger (or weaker) illusory contour formation.

Since the introduction of illusory contours by Schumann in 1904, research in the monocular, static domain has centered on two basic types of of inducers of this illusion. The first type, typified by the displays of Kanizsa (1955), consists of solid inducing elements containing gaps consistent with an occluding figure of the same luminance as the background (Figure 1a). Completion of the illusory contour occurs collinear to supporting edges of the inducers, and we thus refer to this class of stimuli as "edge type". The second class of inducers consists of thin, inducing lines perpendicular to the illusory contour as in an Ehrenstein figure (Ehrenstein, 1941) or a phase shifted line grating (Coren 1972), and thus will be called "line-end type" (Figure 1b). The fundamental question of our study is whether mechanistic differences exist in the processing of these two types of inducers: edges and line-ends. The models of Finkel and Edelman (1989), Grossberg and Mingolla (1985a,b; 1987a,b), Kellman and Shipley (1991), and Peterhans *et al.* (1986) make different predictions in this regard, as we will explain. While illusory contours formed by edge inducers almost invariably have greater support ratios than those formed by line-ends, the latter often have a greater number of discrete regions of support, as Figure 1 indicates.

The juxtaposition of two such familiar figures as those in Figure 1 implicitly frames a deep question, one which has to date received inadequate attention in the literature. Do the two types of inducers differ fundamentally, so that distinct perceptual processes measure their contribution to illusory contour formation on separate dimensions, or are they extremes on some unitary dimension? If the latter, how are values on that dimension related to strength of illusory contour induction? Grossberg and Mingolla (1985a,b, 1987a,b) propose that the boundary completion process that underlies illusory contour formation is intrinsically one of linkage of activity among neural units of similar orientational tuning along a direction that is roughly collinear with the orientational tuning of the inducing units. Their approach handles line-end induction, such as in Figure 1b, by asking: "How can the end of a thin vertical line function as a (fat) horizontal edge?" The mechanism for the generation of "end cuts," reviewed later in this paper, produces signals in orientations roughly perpendicular to the line end that are then treated in the same manner as signals generated directly from horizontal image contrasts for the purposes of boundary completion.

The stances of Kellman and Shipley (1991), Finkel and Edelman (1989) and Peterhans *et al.* (1986) to the question of the relation of edge and line-end inducers differ strikingly from that of Grossberg and Mingolla. In these approaches the *primary* determinant of illusory contour formation is the aligned termination of two or more contours that are themselves perpendicular to the induced illusory contours. (See Figure 2.) The length or orientation of fat edges that are collinear with induced illusory contours may be an important *modifier* of induced brightness or illusory contour saliency, but the collinear edges are not logically treated as inducers as such.[1] Only line-ends or spatial discontinuities, such as corners of luminance contours, play this role in contour formation.

That the few existing computational models dealing with illusory contour formation should have such different assessments of the fundamental relation of edge and line-end inducers spurred us to conduct an empirical investigation of relative efficacy of each inducer in contour formation and brightness induction. Our strategy was to construct figures with varying degrees of line-end and edge induction by making inducing lines (curves) thinner or thicker. For displays on a video display screen, a thin vertical line is rendered as a column of (approximately rectangular) pixels. Treating this as the thinnest line in our experiment, thicker lines were generated using additional adjacent columns of pixels. As a vertical line grows thicker by this procedure, however, the horizontal bottom becomes more edge-like on larger and larger scales. That is, a receptive field tuned to horizontal image contrasts would be directly stimulated at the end of the vertical line. By systematic exploration of families of illusory contour displays with differing proportions of line-end or edge induction, we hoped to better understand the functional roles of the two types of inducing elements.

Concentric ring stimuli

In 1971 Varin presented a stimulus similar to the one depicted in Figure 3, converting standard edge type inducers of a Kanizsa square to a number of line-end inducers by replacing them with partial concentric circles. Several researchers have since reported on the relative strengths of this type of illusory contours with respect to similar stimuli with solid inducers. Halpern (1981) studied solid and concentric Kanizsa figures, finding similar illusory contour clarity and figure brightness for the two types of figures. In a comprehensive comparison between a variety of configurations which give rise to illusory contours, Halpern, Salzman, Harrison, and Widaman (1983) found a Kanizsa square with six-ringed inducers

[1] In a poster presented at the 1992 European Conference on Visual Perception in Pisa, Heitger, von der Heydt, Rosenthaler, Peterhans, and Kubler (1992) presented simulations of illusory contour formation that employ a modification of the Peterhans *et al.* (1986) model that is closer to the Grossberg and Mingolla (1985a,b) model than to that of Peterhans *et al.* Specifically, "para" groupings along the direction specified by the orientations of edges are employed along with "ortho" groupings perpendicular to line ends. Para and ortho groupings appear to be computed as separate quantities, however, and are pooled for the purposes of completion in proportions set by a free parameter – unlike the case in the Grossberg and Mingolla model, where network dynamics determine the strength of perpendicular induction of groupings at line ends.

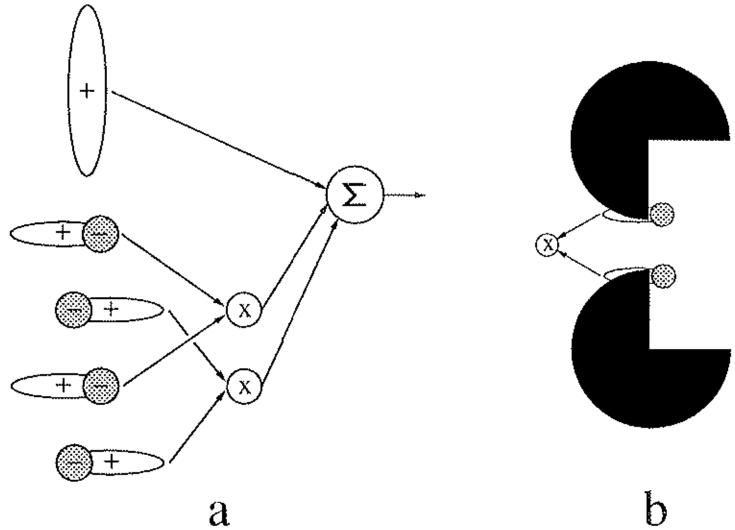

Figure 2: **(a)** In the model of Peterhans, von der Heydt, and Baumgartner (1986) signals for real and illusory contours additively converge at the same neuron (Σ neuron). Illusory contours are generated by endstopped cells that lie along a line perpendicular to their preferred orientation. Pairs of these cells multiplicatively gate one another before progressing to the unified real/illusory representation at the Σ neuron. **(b)** End-stopped cells respond to the corners in a Kanizsa figure leading to illusory contour formation. (Adapted with permission from Peterhans & von der Heydt, 1989)

had a significantly lower clarity than a display with comparable solid inducers. Warm, Dember, Padich, Beckner, and Jones (1987) found the two types of inducers comparable in efficacy over a range of illuminations. In addition, evidence suggests that concentric ring inducers can result in significantly greater illusory brightening effects than their solid counterparts (Frisby & Clatworthy, 1975; Varin, 1971).

The concentric ring Varin figure provides us with a vehicle for testing the relation between line-ends and edges. Specifically, we can study the effect of varying the number of lines and the widths of these lines to determine the relative contributions of these factors to the strength of illusory contours and the brightness of illusory figures. Figure 4 provides examples of the type of stimuli used in our experiment. As described in detail in the Gen-

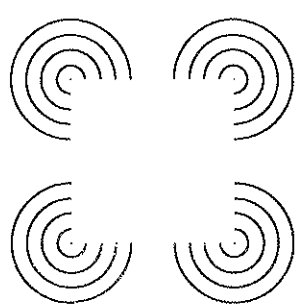

Figure 3: Varin's line-end counterpart to the Kanizsa square

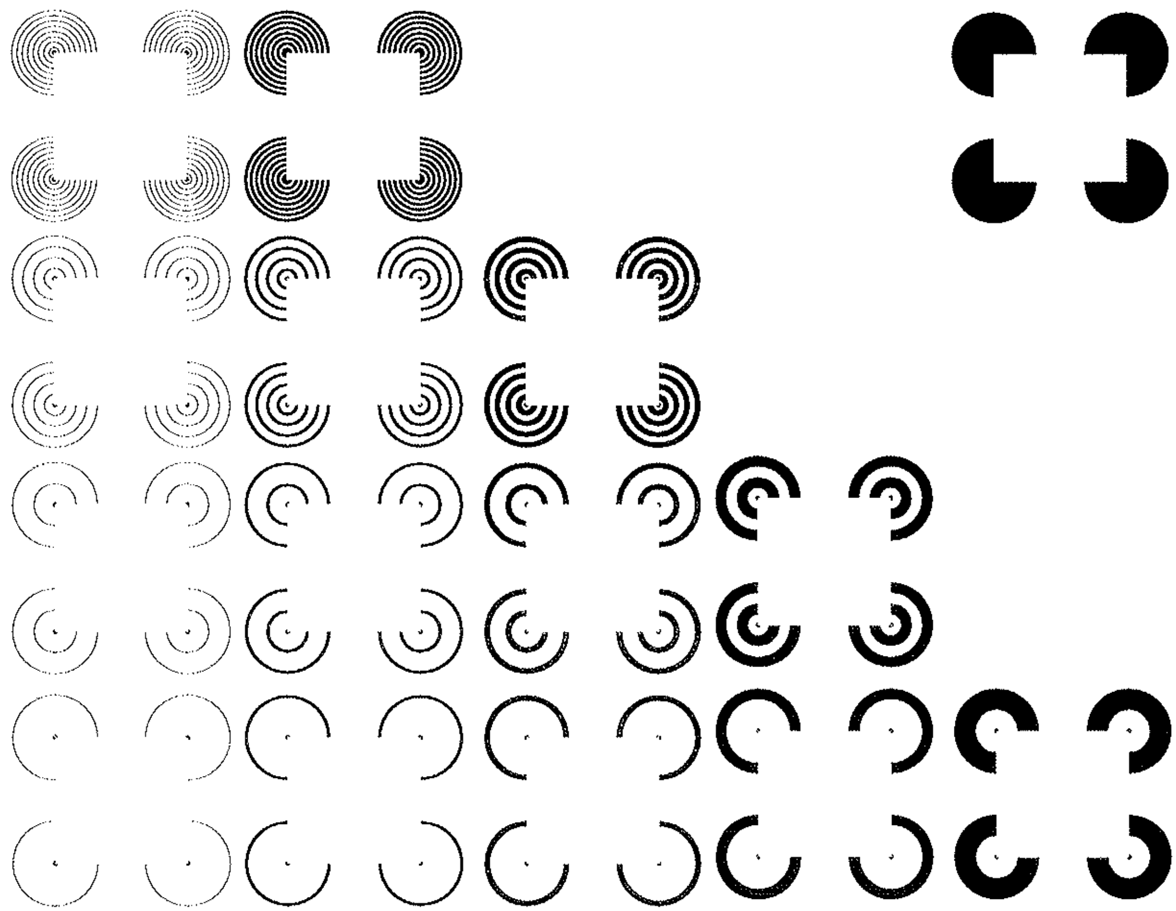

Figure 4: Examples of stimuli employed in the experiment. Actual stimuli were produced on a computer monitor whose pixel resolution, 1280 by 1024, was coarser than the resolution of the laser printer used to generate these images. Line widths, number of lines, and stimuli size (not depicted) were systematically varied.

eral Discussion section, the models of Finkel and Edelman (1989), Grossberg and Mingolla (1985a,b), Kellman and Shipley (1991), and Peterhans *et al.* (1986) predict different effects for these types of configural variations. Although Finkel and Edelman, Kellman and Shipley, and Peterhans *et al.* do not treat the issue of the thickness of lines explicitly, their articles appear to treat thin lines as if they possess a single discontinuity at their ends and thick lines as if they possess discontinuities at each corner of their ends. Altering the width of lines should have little effect on perceived clarity or brightness, according to the line-end or discontinuity models, until the lines are so thick that they have two functional corners (or discontinuities). We can construct pairs of stimuli which have all their discontinuities in the same absolute positions but different edge lengths, as Figure 5 indicates. If discontinuities are indeed the only contributing factor to illusory contour formation, then comparisons of clarity between these "discontinuity equivalent" pairs provide a direct test of the theory. In addition to this type of equivalence, we also may observe sets of "figural equivalent" stimuli which differ only in retinal size, thus allowing us to determine the validity of Shipley and Kellman's (1992a) support ratio hypothesis for non-solid inducers.

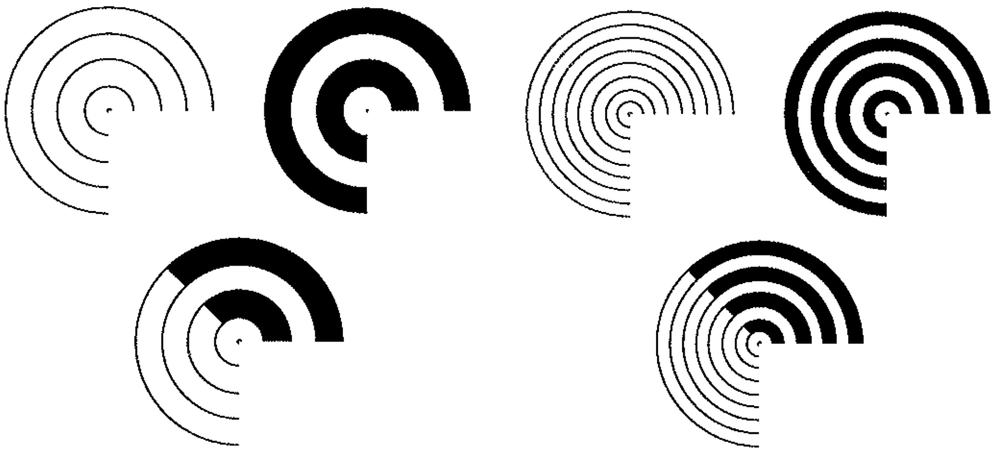

Figure 5: Inducing elements are said to be "discontinuity equivalent" if discontinuities – line-ends and corners – fall in exactly the same place. Two pairs of such stimuli are shown in this figure, with the compound of each pair shown below to indicate the equivalence.

Psychophysical studies of illusory contour strength

Petry, Harbeck, Conway, and Levey (1983) performed a parametric study similar to ours. As in our experiment Petry *et al.* varied the number and width of inducing lines to determine the effect of such changes on the clarity and brightness of the resulting illusory figure. Rather than Kanizsa figures (Figure 1a), however, the researchers employed Ehrenstein figures (Figure 1b). Petry *et al.* found that illusory brightness was an increasing function of the number of inducing lines, while at the same time being an inverted-U function of support ratio (called "area" by the researchers). That is to say, a certain support ratio (approximately 0.4) yielded the brightest illusory figures and increasing the number of lines while maintaining the same support ratio produced increased brightness. Clarity was found to have significantly different dependencies than brightness. While the number of lines had very little effect on the clarity, the support ratio had a positive correlation with the clarity. Clarity increased with support ratio until about 0.4, at which point it leveled out and remained constant. Note that this clarity function differs from the linear relation observed by Kellman and Shipley (1992a) using edge inducers. In another study with Ehrenstein figures, Sambin (1985) found clarity to be partially dependent on the number of lines, monotonically increasing with this parameter to eleven lines, the largest number tested. Petry *et al.* (1983) do note that clarity is somewhat dependent on the number of lines when they are extremely thin, a fact which may reconcile these two findings since Sambin's lines were roughly one third as thick as the thinnest of Petry *et al.*

There are fundamental differences between our experiment and that of Petry *et al.* (1983). While that study was an important parametric investigation, methodological confounds exist in their attempt to measure clarity of *illusory* contours. Using displays such as those of the Petry *et al.* study, if one were to hold the number of lines constant and increase their width, the stimuli would eventually approach a *real* circle as the support ratio approached 1. In our experiment the same limit would result in a standard Kanizsa configuration – still an illusory figure. Petry *et al.* used only a single radius in their experiment, leading to a confounding of the effects of number of lines and line density and between support ratio and absolute amount of support. Clarity measurements by Petry *et al.* were made between the inducing lines, while clarity measurements in our experiment were always within the central gap. The inducers used in their experiments were not strictly lines, but rather lines truncated by the inner circular region such that thick lines had a clear concavity at their ends. No attempt was made by Petry *et al.* to line up corners and line ends in different stimuli to make the stimuli "discontinuity equivalent", and the use of only one size rendered "figural equivalence" impossible to measure.

Experiment 1

Subjects

Five male graduate student volunteers participated in the experiment, ranging in age from 23 to 33 years. These students were familiar with illusory figures, although all were naive to the purposes of the experiment. All observers had normal or corrected-to-normal vision.

Stimuli

Experiments were conducted on a Sun color monitor driven by a Sun SPARCstation 2. Observers were seated comfortably approximately 1.5 meters from the screen. Observations were binocular with observers allowed to move their head and eyes freely. Stimuli were presented in the center of the screen with a mean background luminance of 4.10 cd/m^2 and a 300 to 1 contrast of background to stimulus. The maximum variation in mean luminance due to changes in line width was under 7 percent.

Each display consisted of four concentric-ring pacmen with varying number of lines and line widths, examples of which are given in Figure 4. Three stimulus sizes were employed, with inducer radii of 27', 55', and $1^{\circ}50'$, corresponding to radii of 32, 64, and 128 pixels. The gap between inducers was always equal to the radius, leading to illusory squares of side $1^{\circ}22'$, $2^{\circ}45'$, and $5^{\circ}31'$. For each radius inducers with 1, 2, 4, 8, 16, and 32 lines were employed with widths of $0.9'$, $2.6'$, $4.3'$, $7.8'$, $14.7'$, $28.5'$, $56.2'$, and $1^{\circ}50'$, corresponding to pixel widths of 1, 3, 5, 9, 17, 33, 65, and 129. In addition, each inducer contained a very small "anchor" pacman of $2.6'$ diameter (3 pixels) to aid in corner localization (Day & Jory, 1980; Minguzzi, 1987). Every combination of line width and number of lines was used for each radius, contingent on the particular pair being possible without line overlap or significant aliasing, caused by drawing arcs on a rectangular pixel grid. This implies that for larger radii, more and thicker lines were used. These criteria led to a total of 62 stimuli. Note that the line widths in pixels are powers of two plus an additional one in order to ensure that the ends of thin lines lay in the same position as the corners of thick lines (as in Figure 5) in the quantized monitor display. The above combinations led to 15 distinct discontinuity equivalent pairs in which line "corners" in the same locations and 15 figural equivalent triplets which differed only in retinal size.

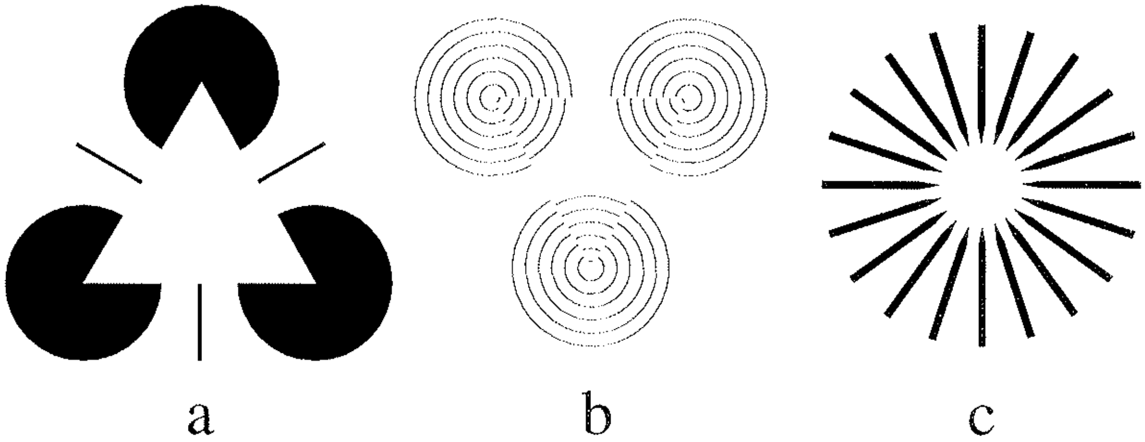

Figure 6: Stimuli employed in the instructions to observers

Procedure

Observers were provided with the following instructions and visual aids for the clarity judgement task:

> You will be presented with a number of stimuli and asked to rate the strength of a particular feature. Before you begin the actual experiment, several example stimuli will be shown in order to help define the feature that you will be asked to rate. [Figure 6a displayed] Many observers perceive a triangle in the center of this display. Even though there are no real luminance gradients along parts of the boundary of this triangle, it may be seen to have continuous sharp edges and may also appear brighter than the background.
>
> You will be shown stimuli similar to this and asked to rate the "clarity" of the contour. By clarity is meant the sharpness or crispness of the edge of the figure. Note that clarity is different from "brightness", as the next two figures will help to illustrate.
>
> [Figure 6b displayed] In this figure you may also perceive a triangular form. While the edge of the form has a certain degree of clarity, you probably will not perceive the triangular form as noticeably brighter than the background. Many observers would give this figure a low brightness rating and an intermediate clarity rating.
>
> [Figure 6c displayed] You may perceive a circular figure above which is brighter than the background but does not have a distinct border. Many observers would give this figure a low clarity rating and an intermediate brightness rating.
>
> Each stimulus that you are shown will have a square interior region. For each stimulus you will be prompted for a clarity rating. Specifically, you are asked to rate the clarity near the mid-points of the edge of the square. The clarity rating should be a number between 1 and 9, with higher numbers meaning greater clarity. Try to use the entire range of values over the course of the experiment. Ignore variations in brightness of the figure and rate only the clarity of each figure's edge.

For the brightness estimation task, the following substitutions were made:

[In place of the 2nd paragraph above] You will be shown stimuli similar to this and asked to rate the "brightness" of the figure with respect to its background. The sharpness or crispness of the edge of the figure is referred to as its "clarity". Note that brightness is different from clarity, as the next two figures will help to illustrate.

[In place of the 5th paragraph above] Each stimulus that you are shown will have a square interior region. For each stimulus you will be prompted for a brightness rating. That rating should represent the brightness of the entire square region. The brightness rating should be a number between 1 and 9, with higher numbers meaning greater brightness with respect to the background. Try to use the entire range of values over the course of the experiment. Ignore the variations in clarity of the figure's edges and rate only the brightness of the square interior region.

After verbally ascertaining that the observers understood the instructions thoroughly, each observer progressed through the 62 stimuli at his own pace, with a 1.5 second blank display between each estimation. Observers typically took less than 15 minutes to accomplish the 62 estimations, after which the process was repeated three more times, with the estimated feature being switched from clarity to brightness (or vice versa) each time. The initial feature was alternated between observers. Four such sessions, spaced over four days yielded eight repetitions each for clarity and brightness.

Results and discussion

All observers showed similar distributions of responses across tasks and conditions. In the ANOVAs with more than two degrees of freedom for experimental factors shown in Tables 1 and 2 or reported in the text, between subject variance was never more than 40and was typically much less. Figure 7a depicts the pooled mean clarity as a function of the *line density*, defined as the number of lines per unit length within the inducer, for radius 128 pixels, with Figure 7b depicting the mean clarity for a single observer along with bars indicating the standard error. Each line in these plots indicates a constant line width, leading to a family of overlapping curves. The corresponding curves for radii of 32 and 64 pixels have the same inverted-U structure, with Figure 7c showing the position of the optimal line density for each radius – the position of the inverted-U peak. Repeated measures F ratios were computed for differences in line density for each of the curves in Figure 7a, and all showed statistically significant differences in clarity ratings across density conditions ($p < 0.005$ for all comparisons). Two out of five of the corresponding comparisons were statistically significant for radius 64 displays. None of the comparisons for radius 32 displays were statistically significant, though the curves contained far fewer data points for this condition. Table 1 indicates all the F ratios for both clarity and brightness with line density as the variable factor and line width and radius held constant. *The inverted-U shape of these curves indicates that for ratings of clarity there is an optimal number of lines* (i.e. more is not always better). The optimal line density decreases with increasing stimuli scale, but not so much as to remain consistent with a scaling hypothesis in which stimuli differing only in magnification would have constant clarity. For example, while the radius quadruples, the optimal density only halves, where such a hypothesis would predict a quartering. The optimal density at the smallest radius occurs when there are two lines spaced $14.7'$ apart, while at the largest radius the optimal clarity is observed

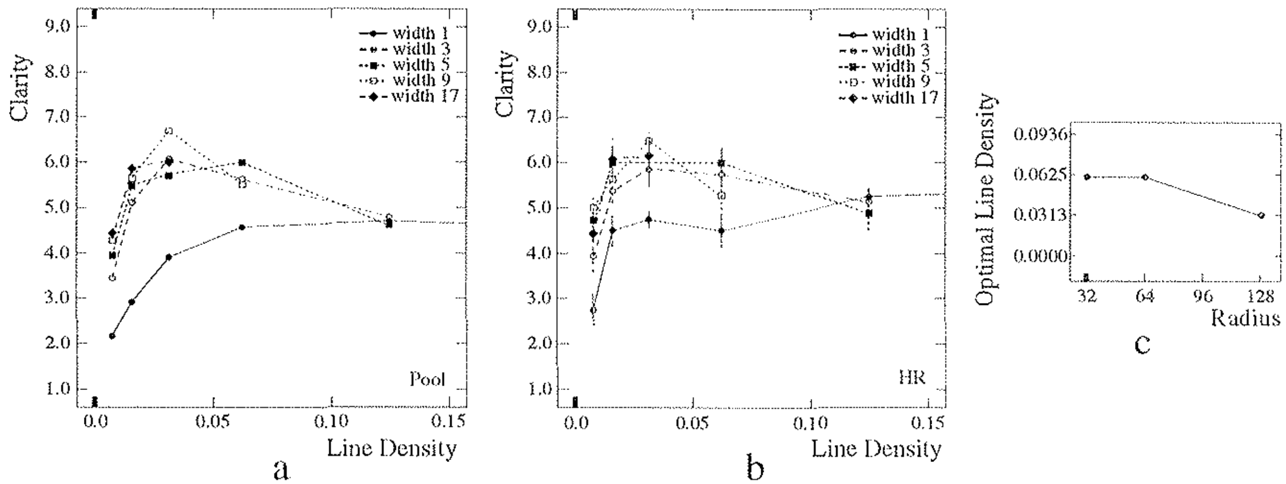

Figure 7: **(a)** Clarity as a function of line density, pooled over five observers, at radius 128 pixels **(b)** Clarity as a function of line density for a single observer (HR) at radius 128 pixels. Bars indicate the standard error. **(c)** Optimal line density as a function of inducer radius

with four lines spaced at $28.5'$. Note that for the thinnest line (width of 1 pixel), clarity continues to increase to the highest density measured, a trend which holds over all radii.

Figure 8a displays pooled mean clarity ratings as a function of line width at radius 128 pixels, with number of lines held constant. (Figure 8b plots means for one observer). While the overlaid curves of the line density plot (Figure 7) might seem to indicate a minimal width effect, this method of displaying the data reveals that clarity ratings gradual increase to a plateau with increasing width, as in the experiments of Petry *et al.* (1983). Differences in mean clarity ratings across widths were statistically significant ($p < 0.05$) for comparisons at all radii for most individual plots with more than two widths. The F ratios for clarity and brightness with line width as the variable factor and radius and line density held constant are provided in Table 2.

Support ratio had an effect on clarity, yielding inverted-U curves with increasing ratio, but a strong effect of number of lines and radius eliminates the simple linear increase in clarity which Kellman and Shipley (1992a) observed with increasing support ratio. The effect of radius can be observed in that of 15 figural equivalent triplets, differing only in retinal size, differences in mean clarity were statistically significant ($p < 0.05$) in 6 cases (primarily in those with few lines), all in the direction of decreasing clarity with increasing radius. Indeed, there was a decrease in *mean* clarity with increasing stimulus scale (radius), a finding supported by the work of Dumais and Bradley (1976). In short, *clarity is not constant for constant support ratio when the support is composed of multiple line ends.* The optimal inducer had radius 128 pixels, 4 lines of width 9 pixels for a clarity rating of 6.7, much greater than the 4.875 rating for the solid inducer figure of the same radius.

Table 1: ANOVA – Clarity and brightness for line density factor

Radius	Line Width	Degrees of Freedom	Clarity F Ratio	$p <$	Brightness F Ratio	$p <$
32	1	$F_{3,12}$	1.6277	–	5.2195	0.025
32	3	$F_{3,12}$	0.8725	–	6.9251	0.01
32	5	$F_{2,8}$	2.1670	–	16.5366	0.005
64	1	$F_{4,16}$	1.7974	–	6.2301	0.005
64	3	$F_{3,12}$	2.7893	–	17.8713	0.001
64	5	$F_{3,12}$	6.0043	0.025	8.0881	0.005
64	9	$F_{2,8}$	7.6458	0.025	20.2235	0.001
128	1	$F_{5,20}$	9.1897	0.001	5.1625	0.005
128	3	$F_{4,16}$	1.3126	0.001	10.6908	0.001
128	5	$F_{4,16}$	7.6088	0.005	11.8324	0.001
128	9	$F_{3,12}$	0.4169	0.005	18.9767	0.001
128	17	$F_{2,8}$	5.5639	0.001	27.2158	0.001

Table 2: ANOVA – Clarity and brightness for line width factor

Radius	Number Lines	Degrees of Freedom	Clarity F Ratio	$p <$	Brightness F Ratio	$p <$
32	1	$F_{5,20}$	11.1240	0.001	4.2378	0.01
32	2	$F_{3,12}$	10.2396	0.005	8.3614	0.005
32	4	$F_{2,8}$	4.8842	0.05	0.6430	–
64	1	$F_{6,24}$	4.0239	0.01	1.7011	–
64	2	$F_{4,16}$	10.6859	0.001	4.9959	0.01
64	4	$F_{3,12}$	3.6030	0.05	1.0079	–
64	8	$F_{2,8}$	0.0039	–	0.2875	–
128	1	$F_{7,28}$	4.5681	0.005	1.1466	0.005
128	2	$F_{5,20}$	6.6206	0.001	2.2083	–
128	4	$F_{4,16}$	5.1665	0.01	3.9239	0.025
128	8	$F_{3,12}$	1.3558	–	2.3042	–
128	16	$F_{2,8}$	0.1169	–	0.0995	–

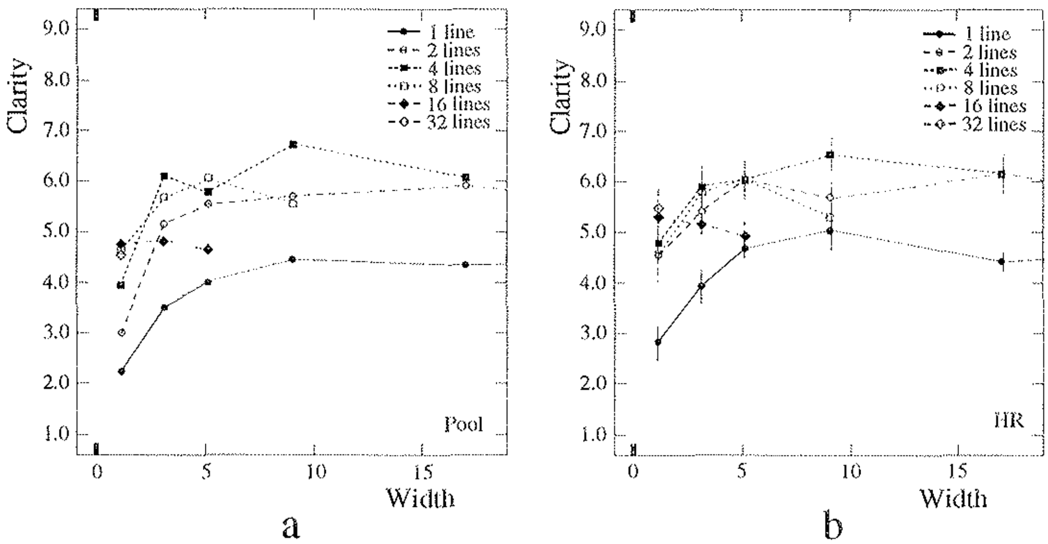

Figure 8: **(a)** Clarity as a function of line width, pooled over five observers, at radius 128 pixels **(b)** Clarity as a function of line width for a single observer (HR) at radius 128 pixels. Bars indicate the standard error.

The equivalent line density brightness plots are shown in Figure 9. Note the high correlation between clarity and brightness, as reported often in the literature (Petry *et al.*, 1983; Watanabe & Oyama, 1988) As with clarity we observe an inverted-U with line density/number of lines. A repeated measures ANOVA verified the effect of line density (Differences for all comparisons with more than two densities were statistically significant, $p < 0.025$). Again, the shift in optimal density observed with changing radius (which is exactly the same as the shift depicted in Figure 7c) is not consistent with the simple scaling hypothesis (differences in figural equivalent cases were statistically significant, $p < 0.05$, in 8 of the 15 triplets), with peaks in brightness occurring at the same line spacings as those in clarity. For brightness the inverted-U is significantly more pronounced and is observed even for the thinnest of lines. The plots of brightness as a function of line width strongly resemble those of the equivalent clarity plots, with the exception of a slight downward trend for large widths. As with clarity the optimal stimulus did not consist of solid inducers (7.175 for 4 lines of width 5 pixels versus 4.375 for solid inducers). Thus the optimal brightness occurs at a specific width and number of lines, with brightness decreasing when either of these parameters varies.

Figure 10 depicts brightness for each radius as a function of support ratio, defined for this stimuli as the line width multiplied by the number of lines and divided by the twice the radius plus the gap, with width held constant. Again we observe little of the monotonic structure reported by Kellman and Shipley (1992a) for clarity with solid inducers, with a clear effect of parameters other than the support ratio and an inverted-U shape for each line-width curve containing 3 or more points. It is interesting to note, however, that a single envelope can encompass the peaks of the curves at all scales. That is, for a given support ratio we can describe the maximum brightness for any scale through reading off the value on a smooth curve linking the plotted peaks, although the particular combination

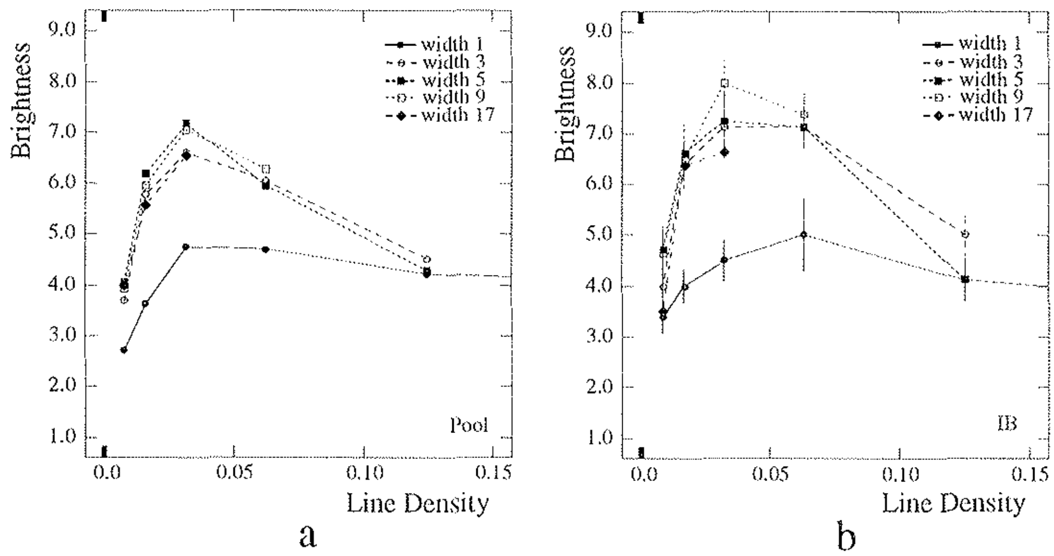

Figure 9: **(a)** Brightness as a function of line density, pooled over five observers, at radius 128 pixels **(b)** Brightness as a function of line density for a single observer (IB) at radius 128 pixels. Bars indicate the standard error.

of number of lines and line widths required to achieve this maximum cannot be easily determined. The implication of this finding is that the support ratio is indeed an important factor, determining the maximum possible brightness of the illusory figure, but not the only factor. Note also that overall mean brightness changed little with changing stimulus size, consistent with the findings of Siegel and Petry (1991).

General Discussion

The data generated in our experiment are not inconsistent with that of Petry *et al.* (1983), but our stimulus manipulations afford several modifications of their conclusions regarding illusory contour induction. Although in our experiment brightness was roughly monotonic with increasing line width, which can be mapped onto support ratio for constant number of lines and radius, it did not increase monotonically with increasing number of lines, as in the Petry *et al.* study. For many widths and radii, brightness started to decrease with more than four lines. The minimum line spacing (maximum density) employed by Petry *et al.* was approximately 17.7 minutes of visual arc, a spacing closer than used for stimuli yielding peak ratings of brightness and clarity ratings in our study at radii of 32 and 64 pixels. Perhaps their line density was not quite high enough to observe the decreasing region of the inverted-U, but more likely this difference resulted from the types of stimuli used in the respective studies. Recall that they used an Ehrenstein configuration whereby the addition of inducing lines would ultimately result in a "real" contour.

The clarity plots generated in our experiment resemble those of Petry *et al.* in that clarity is an increasing function of line width to a saturating limit, but differed in that the number of lines had a significant effect. While our data exhibited a clear inverted-U

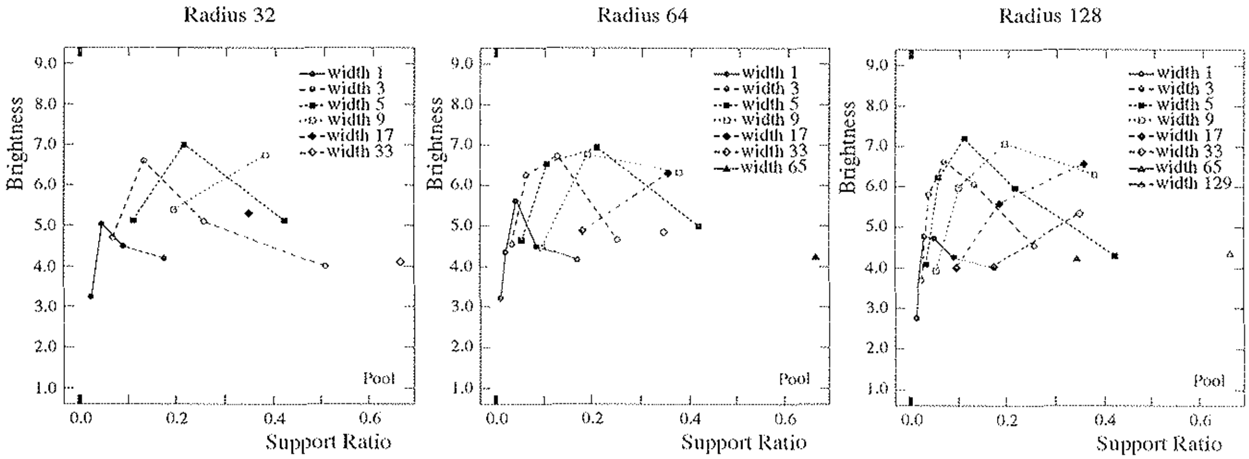

Figure 10: Brightness as a function of support ratio, pooled over five observers, at each radius

with number of lines, theirs appears to be virtually flat. Our clarity data leads to direct tests of the four models mentioned in the introduction. Specifically a model must be able to explain the non-monotonicity of clarity as a function of the number of lines *and* the increase of clarity to a plateau with increasing line width. Before assessing the capacity of the models to explain these data, an account of each paradigm is provided.

The model of Finkel and Edelman (1989) has its roots in a preliminary model sketched out by Peterhans, von der Heydt, and Baumgartner (1986). In the latter model, endstopped cells contribute to illusory contour formation in a direction perpendicular to their preferred orientation, as Figure 2a depicts. Multiplicative gatings of many pairs of endstopped cells lying along the same (perpendicular) line are summed, along with the output of a cell whose preferred orientation lies along this line. In this manner a unified representation of real and illusory contours is generated. Finkel and Edelman (1989) add extra mechanisms to the Peterhans *et al.* model (Figure 11) by first pooling endstopped cell activity over similar orientations at the same location into a "wide-angle" representation, then specifying that termination discontinuities – cues to occlusion – can arise only if at least three such cell pools are active along a line perpendicular to the center (mean) orientation of these wide-angle pools. Finally, perpendicular contour completion between termination discontinuities occurs at the occlusion module. At the termination discontinuity level, activity can be inhibited if the common termination module determines that some of the endstopped activity is actually arising from a natural corner rather than a line termination. Finkel and Edelman claim that their "reentrant" (feedback) system serves to mediate conflicts between real and illusory contours, sharpening or eliminating contours as appropriate. The great importance of line terminations as occlusion indicators for scene segmentation is the basic tenet of Finkel and Edelman's model. The structure of the resulting model mandates that illusory contour formation is mediated only by these terminations. Thus in their model illusory contours formed by edge inducers must result from endstopped activity arising from termination cell activity at the corners of inducing elements, as Figure 2b indicates for the simpler model of Peterhans *et al.*

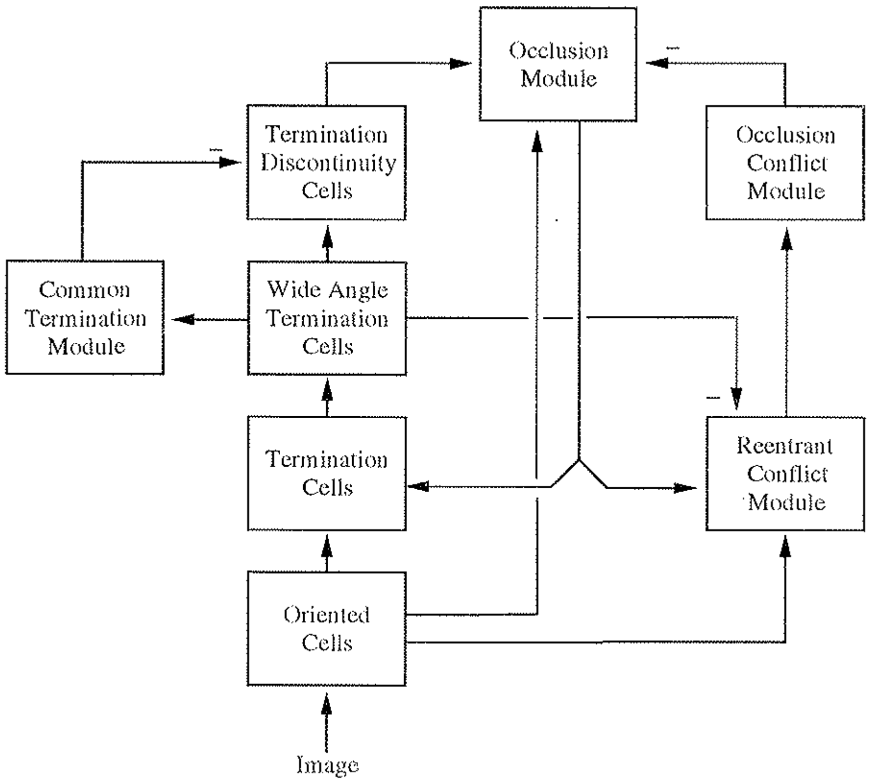

Figure 11: The model of Finkel and Edelman (Adapted with permission from Finkel & Edelman, 1989)

Kellman and Shipley (1991) have taken the line-end argument a step further, claiming first order spatial and spatiotemporal discontinuities as the generating features of illusory contours. These discontinuities can lead to illusory contour formation if they are "relatable", that is, if they satisfy certain constraints concerning the intersection of the extensions of lines perpendicular to the inducing line or corner, as indicated by Figure 12. The degree to which discontinuities are relatable determines the contour strength, a hypothesis supported by several recent experiments (Shipley & Kellman, 1992b). As in the Finkel and Edelman model, edge type illusory contours are induced by the discontinuities at the corners of the inducing elements (Figure 2b). Shipley and Kellman (1992a) present data indicating that contour clarity is a linear function of the support ratio over a range of 0.3 to 0.8, where the length of the supported region and the length of the unsupported region were varied independently. Banton and Levi (1992) report a monotonic, but non-linear, relation. By scaling the size of their stimuli, with inducers and gaps increasing proportionately, Shipley and Kellman showed that clarity is a fixed function of support ratio over a range of absolute stimulus sizes. Their support ratio theory holds that for a given illusory figure size, more support results in higher clarity. Shipley and Kellman note that altering the retinal size of a stimulus has no bearing on its clarity since the support ratio is preserved, a finding at odds with that of Dumais and Bradley (1976), who found decreasing clarity with increasing retinal size. However, Dumais and Bradley used a significantly larger range of retinal sizes than Shipley and Kellman, with an overlap only at the two smallest sizes. A

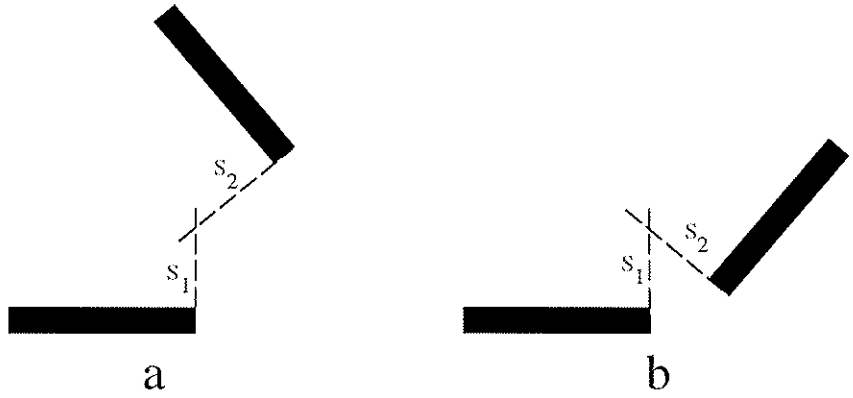

Figure 12: In the model of Kellman and Shipley (1991) illusory contour formation only takes place if the inducing discontinuities are relatable. This occurs when the extensions s_1 and s_2 of the lines perpendicular to the discontinuity intersect with an oblique angle, such as they do in **(a)**. There is no relatability in **(b)** because the intersection of s_1 and s_2 is acute. (Adapted with permission from Kellman & Shipley, 1991)

related property, whereby neural units interact with other neural units in a topographically mapped array over distances that are proportional to the degree of "fan-in" of inputs to the units themselves is referred to as *self-similarity* by Grossberg (1987). In other words, cells "responsible for" responding to properties such as oriented contrast in small regions may interact with other like cells over small neighborhoods, where cells responding to oriented contrast in large regions may interact with their counterparts over correspondingly larger neighborhoods. Shipley and Kellman (1992a; Kellman & Shipley, 1991) note that the support ratio should be incorporated into the mechanics of the illusory contour interpolation process, but provide no further computational details.

Grossberg and Mingolla (1985a,b, 1987a,b) propose the existence of two parallel systems, a Boundary Contour System (BCS) responsible for establishing boundaries of objects, and a Feature Contour System (FCS) for establishing the color and brightness of these objects. The BCS represents the orientation of boundaries at every position and thus it is within the BCS that the completion required for illusory contour formation occurs. It should be noted that in Grossberg and Mingolla's approach the visibility of illusory figures, including induced brightness, involves the FCS as well. As Figure 13 indicates, the first stage of the BCS involves an array of oriented contrast detectors at each spatial location. In the second stage, cells with opposite contrast are pooled to yield a contrast independent boundary representation.

Because units ("cells") sensitive to oriented image contrasts may be activated by stimuli falling anywhere within their extended receptive fields, a degree of positional uncertainty is inevitably present in the distribution of responses of fields of such units. This uncertainty becomes acute during the processing of line-ends and corners. For this reason Grossberg and Mingolla posit the existence of competitive mechanisms designed to overcome uncertainties of local measurement. These processes establish "end cuts" at the end of each line – activity at cells with orientation perpendicular to the line. The competition is divided into two stages. In the first competitive stage cells with the same orientational preference in neighboring locations compete, functionally generating "endstopping" in the sense that "survivors" of the competition will tend to respond most strongly to the ends of lines or corners. In the second competitive stage cells at the same location but different orientations compete. End cuts are generated by the combination of these two competitions as follows. Strong vertical activations along the edges of a vertical line inhibit the weaker activations near the line end. In turn, these weakened vertical activations disinhibit horizontal activations near the end of the line, thereby generating the perpendicular end cut.

The final stage in the BCS is that of long range completion. In contrast with the previous researchers, Grossberg and Mingolla believe completion occurs in directions approximately parallel to the orientation preferred by the "inducing" units of the second competitive stage, rather than in directions perpendicular to the orientation preferred by "inducing" endstopped cells. The second competitive stage of the BCS could be said to render "explicit" the perpendicular "potential for completion" at the ends of lines. To accomplish the completion, bipole filters with bowtie-shaped receptive fields take inputs from spatially disparate cells with orientational preferences whose receptive field centers fall roughly along a common line. Field, Hayes, and Hess (1993) have recently referred to such a mechanism as an "association field." A bipole cell only fires if both sides of its receptive field are excited. These cells feed back to earlier stages, providing orientational information to locations where no "bottom-up" signals supported by image contrast exist. Both edge-type and line-end inducers excite oriented cells, but for the former bipole cells use the oriented activity along the edge directly for completion, while for the latter it is the end cuts generated by the first and second competitive stages which are employed for completion. Note that the long range AND completion employed by Finkel and Edelman (1989) can be accomplished by a bipole cell, as can a measure similar to the relatability of Kellman and Shipley (1991).

The interaction between low-level oriented cells in the model of Finkel and Edelman (1989) is purely cooperative in nature. This implies that we should observe no fundamental (qualitative) change in the computation of illusory contour salience as inducing lines approach one another. That is, more and more endstopped cells (and wide-angle pools) become active as the inducing lines get closer to one another. If the lines have significant width then we might also expect oriented cells lying perpendicular to the inducing elements to respond. The completion process does not explicitly take into account the number of active wide-angle pools or termination discontinuity units, but a greater number of active nodes might result in a more robust illusory contour representation at the occlusion module. As line density increases the Finkel and Edelman model appears to predict *at least* a steady level of activity, in contradiction to our data. Since there is no mechanism to incorporate edge information, other than "standard" oriented cells *that play no part in contour completion*, it is also difficult to see how the effect of line width on contour clarity within the central gap can be explained by their model.

Kellman and Shipley's model (1991) is more phenomenological than mechanistically specified, so it is impossible to say exactly how their system would react to increasing line density. A straightforward application of their ideas, however, would seem to indicate

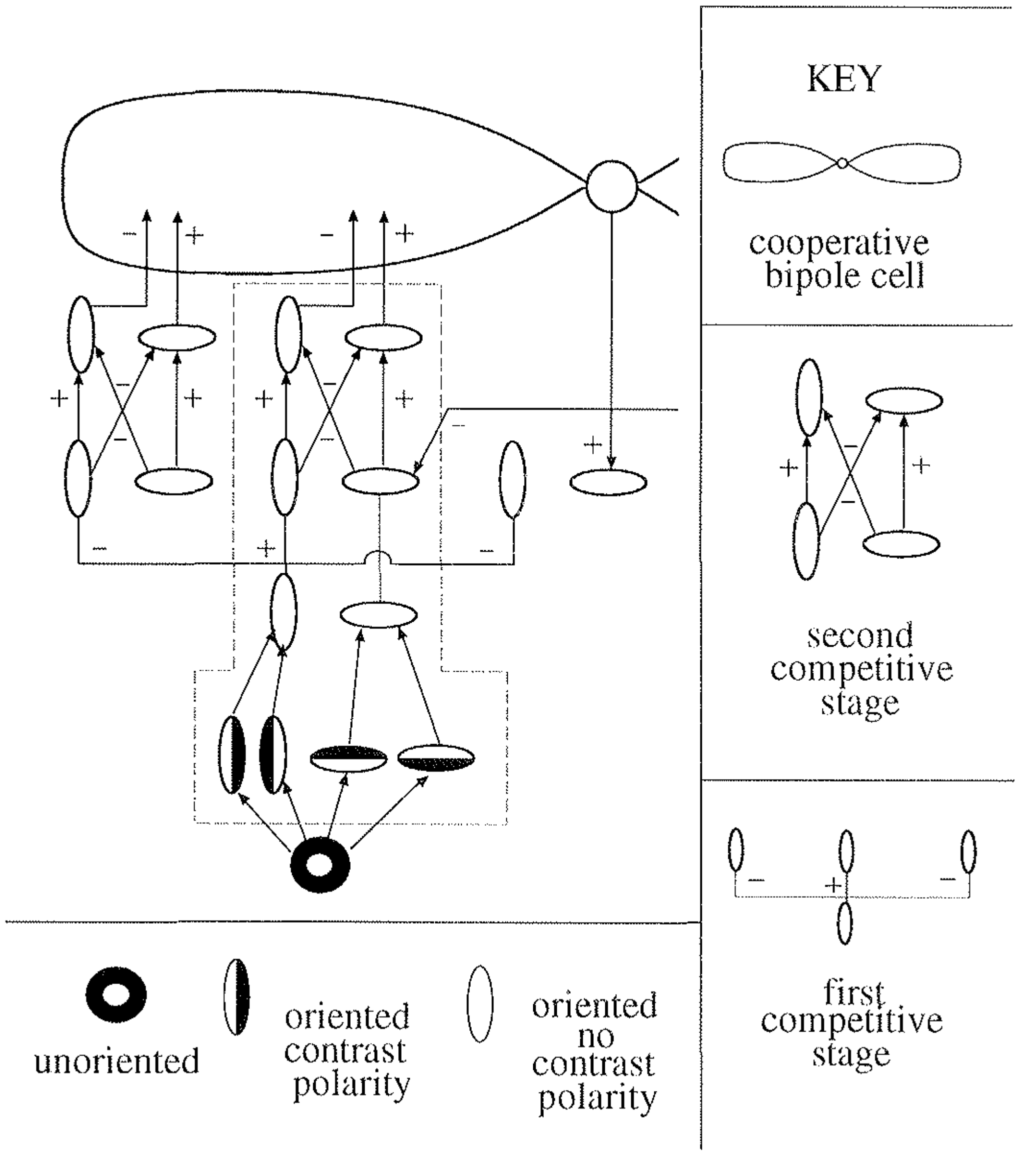

Figure 13: The BCS/FCS model of Grossberg and Mingolla (1985a,b, 1987a,b)

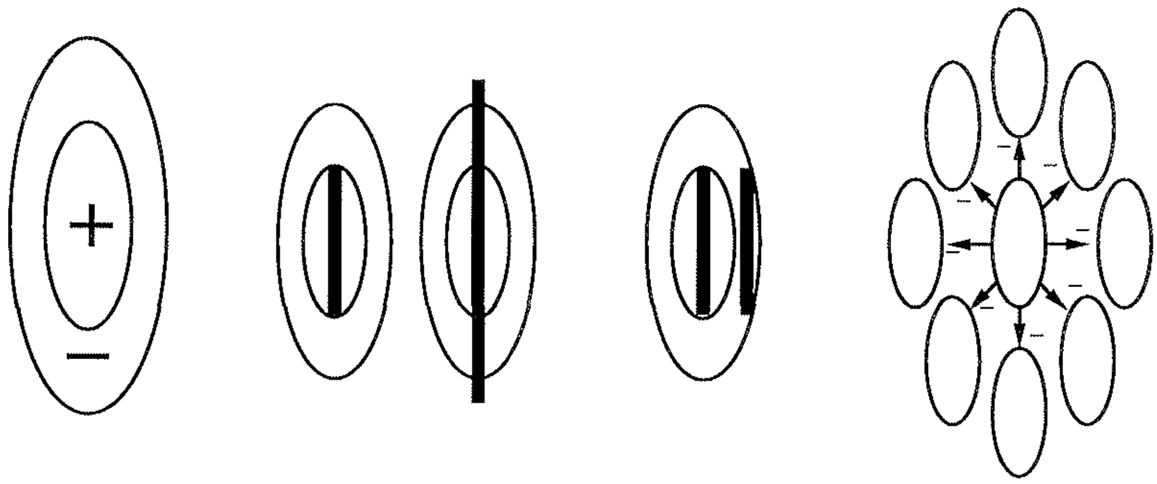

Figure 14: **(a)** In the Dobbins, Zucker, and Cynader (1989) model, endstopping is achieved by subtracting the activity of a cell with large receptive field from a cell with a smaller receptive field having the same orientational preference and position. Compare this with the depiction of the (singly) endstopped cells of Figure 2a, where no inhibition is depicted along the sides of the receptive field. **(b)** Short lines will cause the endstopped cell to respond while extended lines will result in no activity. **(c)** The addition of a short, parallel line impinges on the larger receptive field but not on the smaller, causing a decrease in net activity. **(d)** The first competitive stage of the BCS (Grossberg & Mingolla, 1985a,b) can be viewed as a functionally similar alternative to the mechanism of part (a). Isotropic inhibition between oriented (anisotropic) detectors yields endstopping.

that an increasing number and density of discontinuities should *not interfere with or hinder* contour formation as long as the additional discontinuities occur along the same relatability lines, as in the stimuli of our experiment. Indeed it seems that global relatability would increase as more and more contour information was provided. The linear, monotonically increasing relation between contour clarity and support ratio claimed by Kellman and Shipley (1992a) for solid inducers does not, however, hold for our experiment. Instead, clarity is an inverted-U as a function of the support ratio and there is an independent effect of number of lines. That is, figures made up of different combinations of number and thickness of lines (but the same support ratio) often induce different clarity ratings.

One might argue that an inverted-U would result if there were some type of interference in line-end/discontinuity detection due to lines being too close together. Whether interference will occur depends largely on the structure of line-end detector being employed. A line-end detector must by definition have inhibitory lobes which prevent the unit from being active when a line or edge passes completely through its receptive field. Dobbins, Zucker, and Cynader (1989) have proposed a computational model in which endstopping is realized by the inhibition of cells with small receptive fields by those with larger receptive fields located in the same position with the same orientational preference. Figure 14a schematically depicts the receptive field of an endstopped cell resulting from such a process. Note that the actual mechanism employed by Dobbins *et al.* is a non-linear combination of the output of two cells with complex receptive fields, and thus Figure 14a represents a marked simplification of their concept. By subtracting large scale activity from small scale activity, a response occurs for short lines which fall entirely within the smaller receptive field but not for extended lines which pass completely through this field, as Figure 14b indicates. Note that Figure 2a depicts a different conception of endstopping. The issue of relevance to the present discussion is not one of "single" versus "double" endstopping, however. In both cases unit activity will be decreased whenever any stimulus impinges on the inhibitory region of the endstopped cell. Figure 14c, however, shows how, in a model along the lines of Dobbins *et al.* – but *not* in the scheme of Figure 2a – the addition of a neighboring parallel line can decrease unit response. A more explicit lateral inhibition is posited in the derivation of endstopped cells by Heitger, Rosenthaler, von der Heydt, Peterhans, and Kubler (1992). Can this interference effect be used to explain our data?

Remember that the peaks of our inverted-U clarity curves occurred at relatively large line spacings with respect to line widths. Since individual lines are clearly resolvable (i.e. each line appears clear and distinct, in terms of both position and sharpness) there must exist cells with receptive fields sufficiently small to register each line clearly and independently. It seems unlikely, in the Dobbins *et al.* (1989) paradigm, that inhibitory lobes for endstopping at this small scale would extend out to the distances for which we observed interference effects. More probable is that there exist cells of multiple spatial scales (Kingdom & Moulden, 1992; Grossberg & Mingolla, 1985a,b; Watt & Morgan, 1985). Detectors with small receptive fields would be able to resolve individual lines, but neighboring lines would interfere with the response of endstopped detectors with larger fields. If discontinuities and line-ends (and thus illusory contour formation) were determined primarily at the larger scales, then an inverted-U with increasing density might in fact be observed with the Dobbins *et al.* endstopping mechanism.

We can think of the first competitive stage in the BCS of Grossberg and Mingolla (1985a,b, 1987a,b) as a functionally similar alternative to the endstopped detector model of Dobbins *et al.* (1989). Compare Figure 14d, which depicts the first competitive stage of the BCS, with Figure 14a. In the BCS, as parallel lines approach one another, competition between like-oriented cells at neighboring locations would tend to weaken the responses to these lines in the first competitive stage (Figure 14d). The subsequent competition between orientations at the same location would then yield much weaker end cuts than would otherwise occur. Parallel completion would result in less salient contours due to these weaker end cuts. Since the inducing lines are veridically perceived – there are no *visible* interference effects – this process cannot occur at a very small scale and so we must here too invoke the notion of multiple spatial scales of detectors – or rather multiple scales of BCS mechanisms. The interaction between scales in the BCS has been described in discussions of disparity tuning, depth, and figure-ground separation (Grossberg, 1987, 1992). Note that the converse effect of small scale information disturbing contour formation has long been known – inducer features such as the shape of ends of lines can have a profound effect on contour strength (Ehrenstein, 1941; Kennedy, 1988).

The models of Finkel and Edelman (1989), Kellman and Shipley (1991), and Peterhans *et al.* (1986) are insufficient to explain the effects observed in this experiment, while that of Grossberg and Mingolla (1985a,b, 1987a,b) *may* have the necessary mechanisms to explain our experimental data but presently lacks sufficient parametric specification of their interactions. In any case, our data appears to require that interference between parallel lines must occur at some point in any successful model of illusory contour formation. Interference may result either from a competitive mechanism or from the tendency of dense, parallel lines to inhibit endstopped cell activity. Since the discontinuity models include cells whose primary purpose is illusory contour formation, those models could be elaborated to include long range competition between only these endstopped/discontinuity cells. Interference might be observed in illusory contour formation while perception of the inducing lines would remain unchanged.

Badcock and Westheimer (1985a,b) studied the positional repulsion and attraction effects of thin (half a minute of visual arc) parallel lines in vernier hyperacuity and found such lines affect one another over a broad range, with repulsion dominating for separations of over 4 minutes of arc, and attraction dominating for like-contrast lines at closer distances. The repulsion was observed to extend out to 12 minutes of separation – the maximum distance they tested. Although the lines used by Badcock and Westheimer were thinner than the thinnest employed in our experiment, their experiments show that there can be interference effects between distant parallel lines, even though the appearance of the lines themselves remains unchanged. It is important to note that the range of line separations over which repulsion effects were observed in the Badcock and Westheimer study overlaps the range of separations between inducing lines in our experiments. It is plausible to assume that similar repulsion effects were present for our stimuli. If the hypothesis of self-similarity (Grossberg, 1987) holds, then repulsion effects for thicker lines may extend even further than the ranges measured by Badcock and Westheimer for thin lines.

The brightness effects observed in conjunctions with illusory figures remain virtually untouched by the modeling community. The role of conventional brightness contrast in establishing illusory brightness has been well studied in the domain of edge type inducers (Brigner & Gallagher, 1974; Halpern, Salzman, Harrison, & Widaman, 1983) but such contrast plays little part with line-end type inducers. As early as 1975 Frisby and Clatworthy were hypothesizing the effect of "brightness buttons" at the ends of lines, a hypothesis taken up by Kennedy (1978a, 1978b, 1988) and others (Day & Jory, 1980; Grossberg & Mingolla, 1985a,b, 1987a,b; Jory & Day, 1979). This effect is often referred to as dissimilation (Jory & Day, 1979). Increment threshold tests by Jory (1987) confirm an increased sensitivity in the region at the ends of lines. Moulden and Kingdom (1989) have posited the existence of a similar dissimilation in explaining White's effect (White, 1979) and proposed a mechanism for accomplishing it. The effect of dissimilation on illusory brightness has been widely accepted, but has yet to find its way into any fully specified models.

The BCS/FCS of Grossberg and Mingolla (1985a,b; 1987a,b) is the only model of the three that directly addresses the problem of brightness, but it provides no mechanism capable of providing the illusory brightening of "buttons" at line ends. Recently, however, Gove (1993) has developed just such a mechanism in his dissertation research on extending

Figure 15: Illusory contour in the absence of luminance discontinuities perpendicular to the direction of completion. The luminance of each inducer falls off in space as a Gaussian function such that background luminance is reached at a distance one-third of the way to the nearest inducer, leaving long central gaps of homogeneous luminance. The gradual fall-off in inducer luminance eliminates the sharp corners which discontinuity-based theories require for edge type completion, as in Figure 2b, yet clear illusory contours are perceived spanning the homogeneous central gaps.

the BCS/FCS architecture.

Dissimilation effects require the existence of orientationally sensitive brightness contrast mechanisms such as the simple version proposed by Frisby and Clatworthy (1975). The non-monotonicity of brightness with increasing line density implies that an interference mechanism similar to that in the clarity case must be present. The strong similarities between clarity and brightness effects – peaks at roughly the same line density – raise the possibility that the same system is responsible for both effects.

Proponents of discontinuity theories might find support in the nearly monotonic increase in clarity to a plateau level observed with increasing line width (for a given number of lines). As a line thickens it progresses from a single functional discontinuity to two discontinuities (corners). For discontinuity models, after a certain thickness no additional width will aid in contour formation since the number of discontinuities is fixed at two. The saturating aspect of our line width plots (Figure 8) is thus consistent with these theories.

Discontinuity theories can also be compared with our data on the subset of stimuli that are discontinuity equivalent (Figure 5). An analysis of the clarity of the 15 discontinuity equivalent via repeated measure ANOVA cases shows statistically significant differences ($p < 0.05$) in 4 cases, with the mean clarity of the wider-lined stimuli *always* being higher than that of its discontinuity partner. It appears, although not unequivocally, that corners and line-ends differ in their efficacy as discontinuities. Although neither Finkel and Edelman (1989) nor Kellman and Shipley (1991) have claimed exact equivalence of such discontinuities, they have made no statements about their relative efficacy, tending to treat them interchangeably. In general, it is clear that strict discontinuities in luminance, in the sense of lines or edges perpendicular to completed illusory contours, are not required for illusory contour formation. Figure 11.1 of Shapley and Gordon (1987) displays a disk of homogeneous luminance on a background containing a shallow gradient, whose luminance exactly matches that of the disk along the latter's vertical diameter. This figure, and a different one involving shallow luminance gradients described in the text of page 177 of Grossberg and Mingolla (1985a), evoke the perception of contour completion in the absence of perpendicular inducing contours, although the objection could be raised that the gap to be completed is narrow. Figure 15, however, depicts long illusory contours that cannot be explained by discontinuity theories. The luminance of each inducer is defined by a Gaussian fall-off in space, such that there are no sharp corners analogous to those of Figure 2b which are capable of triggering discontinuity detectors.

Conclusion

Through experiments involving a parametric study of stimuli consisting of combinations of edge type and line-end inducing elements, we have measured the effects of several configural determinants on illusory contour formation. Both clarity and brightness exhibit an inverted-U with respect to number of lines (and line density) and an increase to a plateau with increasing line width. Although the upward sloping part of the inverted-U as a function of line density is reconcilable with several existing models of illusory contour formation, the downward slope which occurs with further increases in these parameters is not fully explained by any current model. We believe, however, that extensions of the Boundary Contour System of Grossberg and Mingolla (1985a,b, 1987a,b) offer the best possibility of quantitatively fitting our data. Our psychophysical data mandate that any valid model must include interference effects between parallel lines or between those neural units responsible for completion of boundary signals in directions perpendicular to the ends of thin lines. Finally, the significant effect of line width on contour clarity is inconsistent with any model which employs *only* completion perpendicular to inducer orientation.

While investigations of illusory contours have long been dominated by presentations of compelling examples or counterexamples for theories, our study helps to extend the parametric understanding of the processes of illusory contour formation. Computational models of illusory contour formation have only been proposed within the last decade. We believe that the next phase of research should include the parametric testing of these models on analogs of stimuli shown to human observers, so that a deeper understanding of the mechanisms of early vision can emerge.

Acknowledgements

The authors wish to thank Birgitta Dresp, Lothar Spillman, and two anonymous reviewers for helpful comments on an earlier draft of the manuscript.

References

Badcock, D.R. & Westheimer, G. (1985a). Spatial location and hyperacuity: flank position within the centre and surround zones. *Spatial Vision*, 1, 3-11.

Badcock, D.R. & Westheimer, G. (1985b). Spatial location and hyperacuity: the centre/surround localization contribution function has two substrates. *Vision Research*, 25, 1259-1267.

Banton, T., & Levi, D.M. (1992). The perceived strength of illusory contours. *Perception and Psychophysics*, 52, 676-684.

Bradley, D.R. & Petry, H.M. (1977). Organizational determinants of subjective contour: The subjective Necker cube. *American Journal of Psychology*, 90, 253-262.

Brigner, W.L. & Gallagher, M.B. (1974). Subjective contour: Apparent depth or simultaneous brightness contrast. *Perceptual and Motor Skills*, 38, 1047-1053.

Coren, S. (1972). Subjective contours and apparent depth. *Psychological Review*, 359-367.

Day, R.H. & Jory, M.K. (1980). A note on a second stage in the formation of illusory contours. *Perception and Psychophysics*, 27, 89-91.

Dobbins, A., Zucker, S.W., & Cynader, M.S. (1989) Endstopping and curvature. *Vision Research*, 29, 1371-1387.

Dumais, S.T. & Bradley, D.R. (1976). The effects of illumination level and retinal size on the apparent strength of subjective contours. *Perception and Psychophysics*, 19, 339-345.

Ehrenstein, W. (1941). Uber abwandlundgen der L hermannschen helliskeitserscheinung. *Zeitschrift fur Psychologie*, 150, 83-91.

Field, D.J., Hayes, A., & Hess, R.F. (1993) Contour integration by the human visual system: Evidence for local "association field." *Vision Research*, 33, 173-193.

Finkel, L.H. & Edelman, G.M. (1989). Integration of distributed cortical systems by reentry: a computer simulation of interactive functionally segregated visual areas. *Journal of Neuroscience*, 9, 3188-3208.

Frisby, J. & Clatworthy, J. (1975). Illusory contours: curious cases of simultaneous brightness contrast. *Perception*, 349-357.

Gregory, R. (1972). Cognitive contours. *Nature*, 51-52.

Gove, A. (1993). A neural network model of visual segmentation and grouping: Illusory contour formation. Unpublished manuscript, Department of Cognitive and Neural Systems, Boston University.

Grossberg, S. (1987) Cortical dynamics of three-dimensional form, color, and brightness perception: II Binocular theory. *Perception and Psychophysics*, 41, 117-158.

Grossberg, S. (1992) Cortical dynamics of 3-D vision and figure-ground separation by visual cortex. Technical Report CAS/CNS-TR-92-023, Boston, MA: Boston University.

Grossberg, S. & Mingolla, E. (1985a). Neural dynamics of form perception: boundary completion, illusory figures, and neon color spreading. *Psychological Review*, 173-211.

Grossberg, S. & Mingolla, E. (1985b). Neural dynamics of perceptual grouping: textures, boundaries, and emergent segmentations. *Perception and Psychophysics*, 141-171.

Grossberg, S. & Mingolla, E. (1987a). Neural dynamics of surface perception: boundary webs, illuminants, and shape-from-shading. *Computer Vision, Graphics, and Image Processing*, 37, 116-165.

Grossberg, S. & Mingolla, E. (1987b). The role of illusory contours in visual segmentation. In Petry, S. & Meyer, G.E. (Eds), *The Perception of Illusory Contours*, (pp. 116-125). New York: Springer-Verlag.

Halpern, D.F. (1981). The determinants of illusory-contour perception. *Perception*, 10, 199-213.

Halpern, D.F., Salzman, B., Harrison, W., & Widaman, K. (1983). The multiple determination of illusory contours: 2. An empirical investigation. *Perception*, 12, 293-303.

Heitger, F., Rosenthaler, L., von der Heydt, R., Peterhans, E., & Kubler, O. (1992). Simulation of neural contour mechanisms: from simple to end-stopped cells. *Vision Research*, 32, 963-978.

Heitger, F., von der Heydt, R., Rosenthaler, L., Peterhans, E., & Kubler, O. (1992). Simulation of V2 contour mechanisms: Image segmentation, illusory contours, and figure - ground discrimination. *Perception*, 21, Supplement 2, 27.

Jory, M.K. (1987). Increment thresholds in illusory contour line patterns. In Petry, S. & Meyer, G.E. (Eds), *The Perception of Illusory Contours*, (pp. 183-190). New York: Springer-Verlag.

Jory, M.K. & Day, R.H. (1979). The relationship between brightness contrast and illusory contours. *Perception*, 8, 2-9.

Kanizsa, G. (1955). Margini quasi-percettivi in campi con stimulazione omogenea. *Rivista di psicologia*, 7-30.

Kanizsa, G. (1979). *Organization in Vision: Essays on Gestalt Perception*. New York: Praeger.

Kellman, P.J. & Shipley, R. (1991). A theory of visual interpolation in object perception. *Cognitive Psychology*, 23, 141-221.

Kennedy, J. (1978a). Illusory contours not due to completion. *Perception*, 7, 187-189.

Kennedy, J. (1978b). Illusory contours and the ends of lines. *Perception*, 7, 605-607.

Kennedy, J. (1988). Line endings and subjective contours. *Spatial Vision*, 3, 151-158.

Kingdom, F. & Moulden, B. (1992). A multi-channel approach to brightness coding. *Vision Research*, 32, 1565-1982.

Minguzzi, G.F. (1987). Anomalous figures and the tendency to continuation. In Petry, S. & Meyer, G.E. (Eds), *The Perception of Illusory Contours*, (pp. 71-75). New York: Springer-Verlag.

Moulden, B. & Kingdom, F. (1989). White's effect: A dual mechanism. *Vision Research*, 29, 1245-1259.

Peterhans, E. & von der Heydt, R. (1989). Mechanisms of contour perception in monkey visual cortex II Contours bridging gaps. *Journal of Neuroscience*, 1749-1763.

Peterhans, E., von der Heydt, R., & Baumgartner, G. (1986). Neuronal responses to illusory contour stimuli reveal stages of visual cortical processing. In Pettigrew, J.D, Sanderson, K.J., and Levick, W.R. (Eds), *Visual Neuroscience*, (pp. 343-351). Cambridge, MA: Cambridge University Press.

Petry, S., Harbeck, A., Conway, J., & Levey, J. (1983). Stimulus determinants of brightness and distinctness of subjective contours. *Perception and Psychophysics*, 34, 169-174.

Ramachandran, V.S. (1986). Capture of stereopsis and apparent motion by illusory contours. *Perception and Psychophysics*, 39, 361-373.

Rock, I. & Anson, R. (1979). Illusory contours as the solution to a problem. *Perception*, 665-681.

Sambin, M. (1985) Figure anomale: la misura dell'ampiezza di una disomogeneita indotta. In Gerbino, W. (Ed), Conoscenza e struttura: Festschrift per Gaetano Kanizsa, (pp. 437-452). Bologna: Il Mulino.

Schumann, F. (1904). Einige Beobachtungen uber die Zusammenfassung von Gesichtseindrucken zu Einheiten. *Psychologische Studien*, 1-32.

Shapley, R. & Gordon, J. (1987). The existence of interpolated illusory contours depends on contrast and spatial separation. In Petry, S. & Meyer, G.E. (Eds), *The Perception of Illusory Contours*, (pp. 109-115). New York: Springer-Verlag.

Shipley, T.F. & Kellman, P.J. (1990). The role of discontinuities in the perception of subjective figures. *Perception and Psychophysics*, 48, 259-270.

Shipley, T.F. & Kellman, P.J. (1992a). Strength of visual interpolation depends on the ratio of physically specified to total edge length. *Perception and Psychophysics*, 52, 97-106.

Shipley, T.F. & Kellman, P.J. (1992b). Perception of partly occluded objects and illusory figures: Evidence for an identity hypothesis. *Journal of Experimental Psychology: Human Perception and Performance*, 18, 106-120.

Siegel, S. & Petry, S. (1991). Evidence for independent processing of subjective contour brightness and sharpness. *Perception*, 20, 233-241.

Smith, A. & Over, R. (1975). Tilt aftereffects with subjective contours. *Nature*, 257, 581-582.

Smith, A. & Over, R. (1976). Color-selective tilt aftereffects with subjective contours. *Perception and Psychophysics*, 20, 305-308.

Smith, A. & Over, R. (1977). Orientation masking and the tilt illusion with subjective contours. *Perception*, 6, 441-447.

Smith, A. & Over, R. (1979). Motion aftereffect with subjective contours. *Perception and Psychophysics*, 25, 95-98.

Varin, D. (1971). Fenomeni di contrasto e diffusione cromatica nell' organizzazione spaziale del campo percettivo. *Rivista di Psicologia*, 65, 101-128.

Vogels, R. & Orban, G.A. (1987). Illusory contour orientation discrimination. *Vision Research*, 27, 453-467.

von Grunau, M.W. (1979). The involvement of illusory contours in stroboscopic motion. *Perception and Psychophysics*, 25, 205-208.

von der Heydt, R., Peterhans, E., & Baumgartner, G. (1984). Illusory contours and cortical neuron responses. . *Science*, 224, 1260-1262.

von der Heydt, R., & Peterhans, E. (1989). Mechanisms of contour perception in monkey visual cortex. I. Lines of pattern discontinuity. *Journal of Neuroscience*, 1731-1748.

Wallach, H. & Slaughter, V. (1988). The role of memory in perceiving subjective contours. *Perception and Psychophysics*, 43, 101-106.

Warm, J.S., Dember, W.N., Padich, R.A., Beckner, J., & Jones, S. (1987). The role of illumination level in the strength of subjective contours. In Petry, S. & Meyer, G.E. (Eds), *The Perception of Illusory Contours*, (pp. 176-182). New York: Springer-Verlag.

Watanabe, T. & Oyama, T. (1988). Are illusory contours a cause or a consequence of apparent differences in brightness and depth in the Kanizsa square. *Perception*, 17, 513-521.

Watt, R.J. & Morgan, M.J. (1985). A theory of the primitive spatial code in human vision. *Vision Research*, 11, 1661-1674.

Weisstein, N., Maguire, W., & Berbaum, K. (1977). A phantom-motion aftereffect. *Science*, 198, 955-958.

White, M. (1979). A new effect on perceived lightness. *Perception*, 8, 413-416.